# Onset of normal and inverse homoclinic bifurcation in a double plasma system near a plasma fireball

Vramori Mitra, Bornali Sarma, Arun Sarma, M. S. Janaki, and A. N. Sekar Iyengar

Citation: Phys. Plasmas **23**, 032304 (2016); doi: 10.1063/1.4942932
View online: http://dx.doi.org/10.1063/1.4942932
View Table of Contents: http://aip.scitation.org/toc/php/23/3
Published by the American Institute of Physics

# Onset of normal and inverse homoclinic bifurcation in a double plasma system near a plasma fireball

Vramori Mitra,[1] Bornali Sarma,[1] Arun Sarma,[1] M. S. Janaki,[2] and A. N. Sekar Iyengar[2]
[1]VIT University Chennai Campus, Vandalur-Kelambakkam Road, Chennai-600127, Tamil Nadu, India
[2]Plasma Physics Division, Saha Institute of Nuclear Physics, 1/AF, Bidhannagar, Kolkata 700064, India

(Received 8 January 2016; accepted 16 February 2016; published online 4 March 2016)

Plasma fireballs are generated due to a localized discharge and appear as a luminous glow with a sharp boundary, which suggests the presence of a localized electric field such as electrical sheath or double layer structure. The present work reports the observation of normal and inverse homoclinic bifurcation phenomena in plasma oscillations that are excited in the presence of fireball in a double plasma device. The controlling parameters for these observations are the ratio of target to source chamber ($n_T/n_S$) densities and applied electrode voltage. Homoclinic bifurcation is noticed in the plasma potential fluctuations as the system evolves from narrow to long time period oscillations and vice versa with the change of control parameter. The dynamical transition in plasma fireball is demonstrated by spectral analysis, recurrence quantification analysis (RQA), and statistical measures, *viz*., skewness and kurtosis. The increasing trend of normalized variance reflects that enhancing $n_T/n_S$ induces irregularity in plasma dynamics. The exponential growth of the time period is strongly indicative of homoclinic bifurcation in the system. The gradual decrease of skewness and increase of kurtosis with the increase of $n_T/n_S$ also reflect growing complexity in the system. The visual change of recurrence plot and gradual enhancement of RQA variables *DET*, $L_{max}$, and *ENT* reflects the bifurcation behavior in the dynamics. The combination of RQA and spectral analysis is a clear evidence that homoclinic bifurcation occurs due to the presence of plasma fireball with different density ratios. However, inverse bifurcation takes place due to the change of fireball voltage. Some of the features observed in the experiment are consistent with a model that describes the dynamics of ionization instabilities. © *2016 AIP Publishing LLC*.
[http://dx.doi.org/10.1063/1.4942932]

## I. INTRODUCTION

Investigation of the physics of plasma fireball is a topic of broad interest in different branches of plasmas such as space and laboratory plasmas and plasma processing. There has been plenty of research work carried out in the context of plasma fireballs, in particular, the nonlinear behaviour of fireball dynamics in recent years.[1–8] Fireball (FB) is a glowing sheath region around a positively biased electrode and has been first observed during investigations of sheath phenomena.[5] Inverted fireballs, trapped inside spherical electrodes made of transparent grid, were developed for the first time by Stenzel *et al*.[6,7] in an unmagnetized dc discharge to study the characteristic instabilities and nonlinear effects in such fireball configurations.

Formation of sheath is a ubiquitous phenomena in a double plasma system, and it is highly important for its huge contribution to nonlinear effects in plasma oscillations. There have been plenty of research works done on sheath plasma so far.[9–21] Sheath instability is one of the causes of generation of ion acoustic instability. Electrostatic sheath is generated around the mesh grid in a double plasma device because of the plasma potential difference between the chambers and also due to the grid bias voltage. When a positively biased electrode is immersed into the unperturbed and partially ionized plasma, it attracts the electrons and creates an electron rich sheath which generates a luminous quasi spherical space charge region near the electrode named as fireball. Fireball shows highly nonlinear phenomena involving the physics of sheath, double layers, and ionization beams.[22–24] In this paper, investigation has been carried out to study the effect of fireball associated with a plasma density gradient on the dynamics of plasma oscillations.

In the present work, homoclinic bifurcation has been observed in an argon double plasma system. Among different types of bifurcation phenomena, homoclinic bifurcation is one in which the time period of oscillation increases with the increase of control parameter or vice versa. There is a certain scaling behavior between the time period T and the controlling parameter. There have been several works on homoclinic bifurcation including spiking and bursting[25] in the context of chemical,[26] plasma,[27] and laser systems.[28] Recently, normal and inverse homoclinic bifurcation has been studied in a glow discharge plasma system.[29] But to the best of our knowledge, no evidence of homoclinic bifurcation in a double plasma system has been reported yet. In this paper, we report the existence of homoclinic bifurcation in fireball dynamics.

An attempt has been made to understand the experimental findings by using a numerical model based on two fluid equations. A nonlinear dynamical equation describing the temporal variation of density fluctuations and involving ionization and recombination effects is used to model the plasma behaviour. The growth and decay of fireball are known to excite and modulate plasma instabilities.[3] Experimental

 

analysis reveals that plasma potential fluctuations (PPF) undergo a homoclinic bifurcation with the increase in the ratio between the target and source densities. The variation in the densities is modelled through a change in the ionization parameter in the numerical analysis.

An extensive analysis is carried out with the time series obtained from the experiment as well as numerical modeling. The numerical results are qualitatively close to the experimental result (homoclinic bifurcation). The paper is organized as follows. Section II describes the experimental setup used for the experiment. In Section III, the experimental results are discussed. Section IV contains the behaviour of the plasma dynamics for different density ratios at constant fireball voltage. Section V contains the recurrence plot (RP) theory and recurrence quantification analysis (RQA) of plasma oscillations. In Section VI, description of fireball effects at constant density ratio has been included. In Section VII, numerical modelling of the experimental observations has been carried out using a nonlinear equation based on two-fluid model. Section VIII concludes with a brief summary of experimental results and new possibilities of investigation.

## II. EXPERIMENTAL SETUP

The experiment has been performed in a double plasma device consisting of a stainless steel cylindrical chamber of diameter 40 cm and length 90 cm, and it is divided equally into two parts with a stainless steel mesh grid of optical transparency around 83%. Fig. 1(a) shows the schematic diagram of the experimental setup. The two parts of the chamber are considered as source (S) and target (T) plasma, respectively. The base pressure is kept at $1.0 \times 10^{-6}$ mbar by using a diffusion pump backed by a rotary pump. Four tungsten filaments of 0.1 mm in diameter and 60 mm in length are placed in both source and target section at equal distance apart. Ar gas is introduced at $4–8 \times 10^{-4}$ mbar under continuous pumping conditions, and discharge has been struck by introducing a voltage between filament and the chamber. The discharge current at the source chamber is maintained constant at 200 mA, and the discharge current at the target chamber is varied from 180 mA to 20 mA. The plasma density ratio between target and source chamber $n_T/n_S$ have been estimated for each change of target current. Fig. 1(b) shows the target to source plasma density ratio ($n_T/n_S$) as a function of target current.

An additional tantalum electrode (P) of 10 mm diameter is placed on the axis of the system at 25 cm away from the mesh grid in the target section. Back side of the electrode is shielded, so that no ionization can take place in the back side. The electrode is then biased positively from 280 V to 400 V, respectively, depending on $n_T/n_S$ to have a uniform spherical fireball surrounding the front surface of the electrode. When the bias voltage to the electrode exceeds a certain critical value, an additional discharge occurs in front of the anode, and a new layer of plasma with higher potential and density is created. In this case, the fireball plasma is separated from the rest of the plasma by a boundary in the form of a double layer. Plasma oscillations excited by this double layer formation are generally coupled to the internal plasma oscillations and produce several phenomena. The basic plasma parameters are measured by a plane Langmuir probe of diameter 3 mm placed at 15 cm far away from the additional electrode (P). Typical Langmuir probe I-V characteristics for different $n_T/n_S$ at a certain voltage (350 V) supplied to electrode P are shown in Fig. 2(a). The plasma parameters are electron density $n_e = 10^8\,\mathrm{cm}^{-3}$, electron temperature $T_e = 1–2$ eV, and ion temperature $T_i \ll T_e$. The particular striking voltage needed to produce fireball for different ($n_T/n_S$) is shown in Fig. 2(b). Langmuir probe has also been used to measure the electron saturation current fluctuations by biasing it just above the plasma potential. The electron saturation current is obtained from the voltage drop across a 1 kΩ resistance. Plasma potential fluctuations data are acquired at a sampling frequency of 2000 kHz. The obtained data of plasma potential fluctuations are further analyzed with the help of spectral analysis, phase space plot, and recurrence quantification analysis technique for investigating their nonlinear behavior.

## III. RESULTS AND DISCUSSION

The main goal of our experiment is to study the nonlinear behavior of oscillations in potential fluctuations at different values of control parameter in a double plasma system. Initially, plasma density ratio of source and target chambers are considered as the control parameter of the system, and at a particular fireball voltage (voltage applied to the additional electrode), the plasma density in the target chamber is varied by reducing the discharge current while the source current is maintained constant at 200 mA. Complete set of experiments has been divided into 2 parts, *viz.*, study of fireball associated

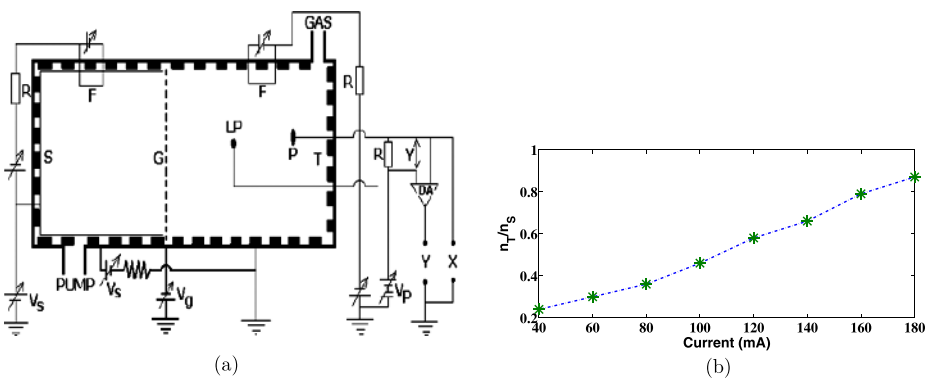


FIG. 1. (a) Schematic diagram of the whole experimental setup. (b) Target to source plasma density ratio ($n_T/n_S$) with respect to different target current: (1) 40 mA, (2) 60 mA, (3) 80 mA, (4) 100 mA, (5) 120 mA, (6) 140 mA, (7) 160 mA, and (8) 180 mA.

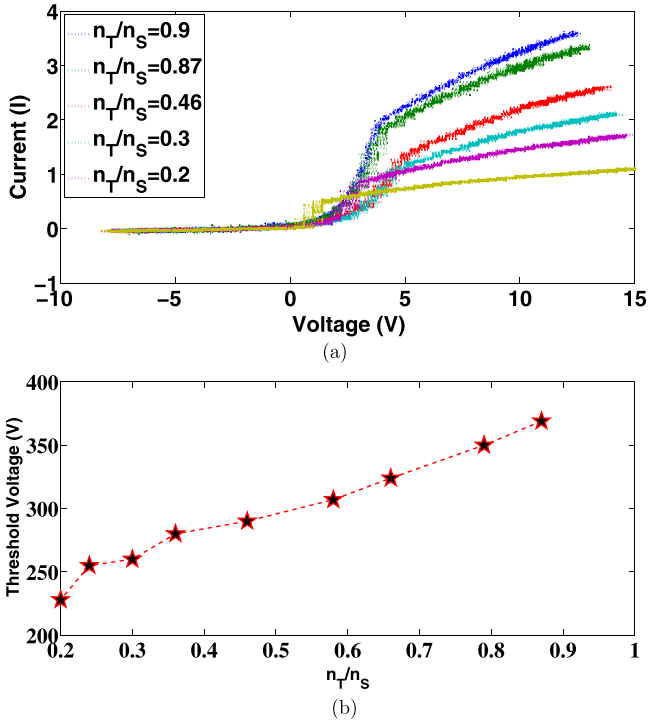


FIG. 2. (a) Current–voltage characteristics, measured by Langmuir probe for different values of $n_T/n_S$. (b) Threshold value of fireball voltage at different density ratio of target to source chamber ($n_T/n_S$).

plasma potential fluctuations with respect to variation in (i) density ratio of target to source chamber ($n_T/n_S$) and (ii) different applied voltages at the electrode for a fixed value of $n_T/n_S$. We have observed the dynamics of plasma oscillations obtained by Langmuir probe when the voltage of the electrode (P) is maintained at 330 V and 350 V. A spherical glowing region, named as fireball, is generated around the external electrode at the respective discharge voltages. Next, at a particular target current, 80 mA ($n_T/n_S$), the voltage of the additional electrode has been varied from 280 V to 330 V to see the effect of the fireball. It has been noticed that variation in the target to source density ratio affects the dynamics of the plasma oscillations in a contrasting way compared to the role of voltage applied to the electrode at a particular value of density ratio. In these two cases, opposite bifurcation scenario have been observed. Voltage applied to the electrode, where fireball is generated and target to source density ratio are seen, play a significant role in the bifurcation of plasma oscillations.

## IV. EFFECT OF $n_T/n_S$ AT CONSTANT FB VOLTAGE

Figs. 3 and 4 show the raw signal of plasma potential fluctuations with respect to $n_T/n_S$, for two different discharge voltages, *viz.*, 330 V and 350 V, respectively. The data point of the length of the raw signal is 2500. The time evolution of the raw signal is shown, with the time scale obtained by the oscilloscope, while acquiring the data. Increasing the value of $n_T/n_S$, one sees the onset of complex periodic oscillations with multipeaked periodic states.[30] In Fig. 3(a), first the initial oscillation shows a large and several small peaked periodic states. By increasing the value of $n_T/n_S$, the amplitude of the large amplitude oscillation diminishes. However, a new large amplitude oscillation appears when the value of $n_T/n_S$ is 0.3, and again, it disappears at $n_T/n_S = 0.58$. Moreover, it has been noticed that throughout all the changes in $n_T/n_S$, the oscillations show the constant presence of large and small peaked periodic states. Similar features are observed in Fig. 4. Initially, a large and several small amplitude oscillations are seen (Figs. 4(a), 4(b), and 4(c)). Increasing the value of $n_T/n_S$, a new large oscillation has been observed (Fig. 4(d)). With a further increase of $n_T/n_S$, the oscillation goes to a broad time period oscillation similar to Fig. 3. However, from the experimental results, it is obvious that the oscillations are periodic by nature initially and gradually with the change of the controlling parameter; the time period between two successive oscillations and the amplitude of the oscillations are also increases.

The time series analysis obtained at 330 V and 350 V for different $n_T/n_S$ clearly shows the homoclinic bifurcation sequence of the signals. It has been noticed that when the value of $n_T/n_S$ is high (0.9), i.e., the target density is almost similar to source plasma density, a relatively high threshold voltage (369 V) is required to generate fireball as shown in Fig. 2(b). However, when $n_T/n_S$ is very less (0.24), fireball appears even at lower voltage, i.e., 255 V. This signifies that the density gradient is playing a vital role for the formation of fireball. Moreover, with high density gradient, since the

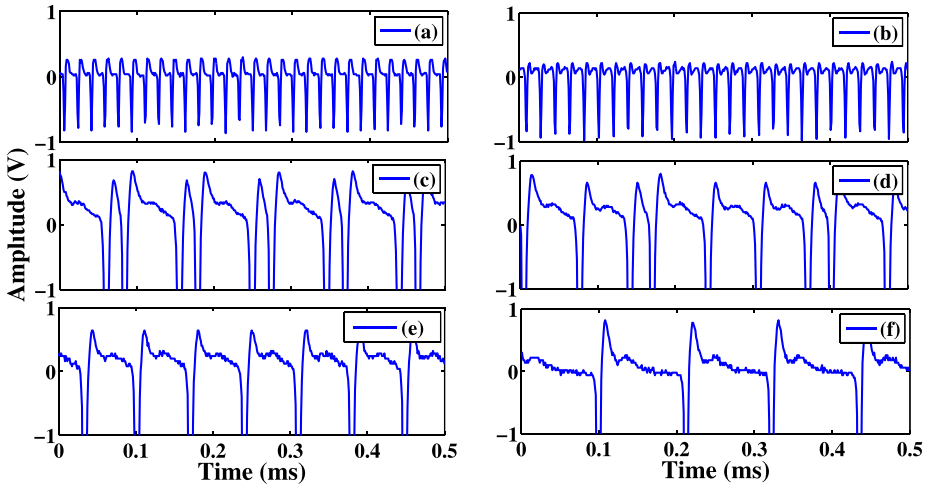


FIG. 3. Time series of plasma potential fluctuations in various $n_T/n_S$: (a) 0.20, (b) 0.24, (c) 0.3, (d) 0.36, (e) 0.46, and (f) 0.58 at 330 V fireball voltage.

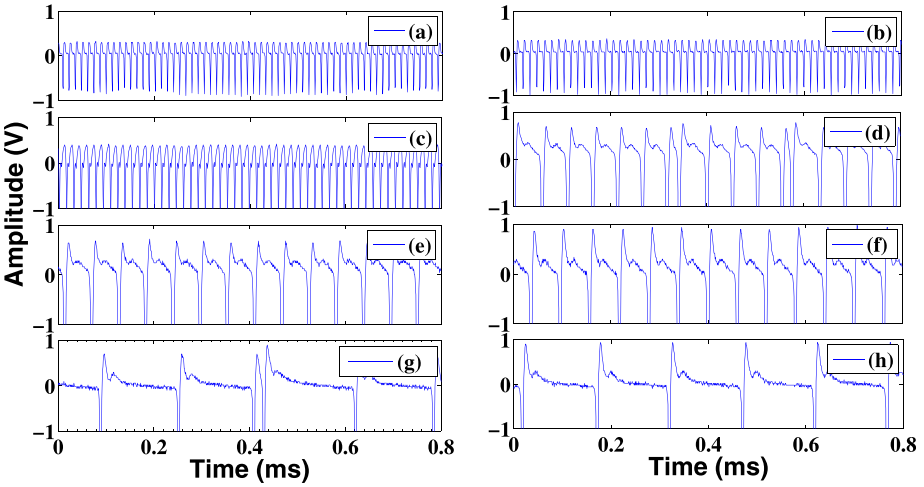


FIG. 4. Time series of plasma potential fluctuations in various target to source density ratios ($n_T/n_S$): (a) 0.24, (b) 0.3, (c) 0.36, (d) 0.46, (e) 0.58, (f) 0.66, (g) 0.79, and (h) 0.87 at 350 V fireball voltage.

potential in the target side is much more than the source side,[31] it requires less voltage to form a sheath region encompassing the electrode.

### A. Normalized variance and Hurst exponent

The normalized variance (*NV*) is widely used to quantify the regularity of the spikes of the signal.[27] It is defined as

$$NV = \frac{std(ISI)}{mean(ISI)},$$

where ISI is considered as the interspike interval between two consecutive spikes appearing in the signal and std is the standard deviation of the data of the signal. Normalized variance is computed for each signal at different $n_T/n_S$ using the above formula with the help of MATLAB software.

Fig. 5(a) reflects the *NV* of plasma potential fluctuations at various density ratio, while fireball voltage is maintained constant at 350 V. It has been noticed that as the $n_T/n_S$ is increased further, the value of *NV* is also increased. The value of *NV* reaches maximum, where the density ratio is high and it represents the irregularity of the spike sequence. In general, for a purely periodic time series, *NV* approaches to zero. At lower density ratio, *NV* exhibits small values approaching zero, which corresponds to the periodic nature of the oscillation. Hence, it is evident that $n_T/n_S$ enhances the irregularity in the dynamics of the plasma oscillations. This is due to the consequence of the density gradient developed in the system with the rise of the $n_T/n_S$.

The Hurst exponent (H) is computed to evaluate the temporal correlation of the time series of plasma oscillations using rescaled range analysis (*R*/*S*) method.[32] The *R*/*S* is characterized as the ratio of the maximal range of the integrated signal normalized to the standard deviation[33]

$$\frac{R(n)}{S(n)} = \frac{max(0, W_1, W_2, \ldots, W_n) - min(0, W_1, W_2, \ldots, W_n)}{\sqrt{S^2(n)}},$$

where

$$W_k = X_1 + X_2 + \cdots\cdots + X_k - k\overline{X(n)},$$

*X(n)* is the data and *n* is the data length. For phenomena characterized by a long-range time dependence, the expected value of *R*/*S* scales as

$$E\left[\frac{R(n)}{S(n)}\right] = \lambda n^H,$$

where *E(x)* is the expected value of the variable *x* and *H* is the Hurst exponent.

The values of $H = 0.5$ indicate that the time series is random in nature, i.e., each event included in the system is

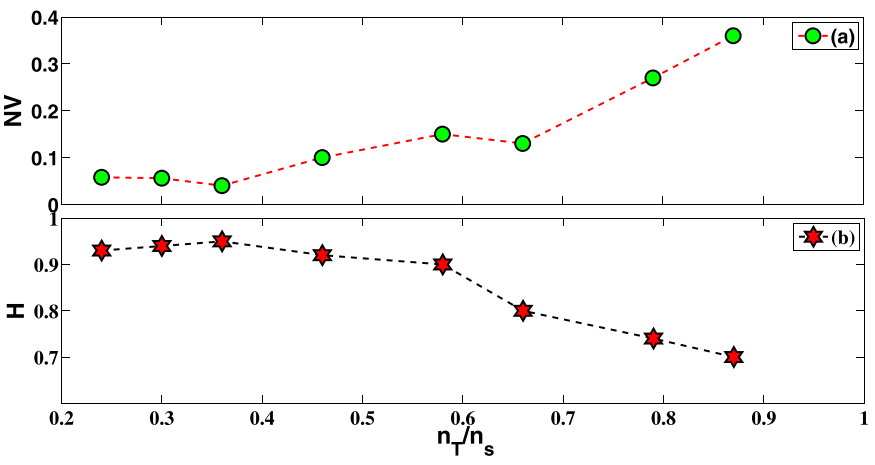


FIG. 5. (a) Normalized variance and (b) Hurst exponent for plasma potential fluctuations at different $n_T/n_S$, while fireball voltage is maintained constant at 350 V.

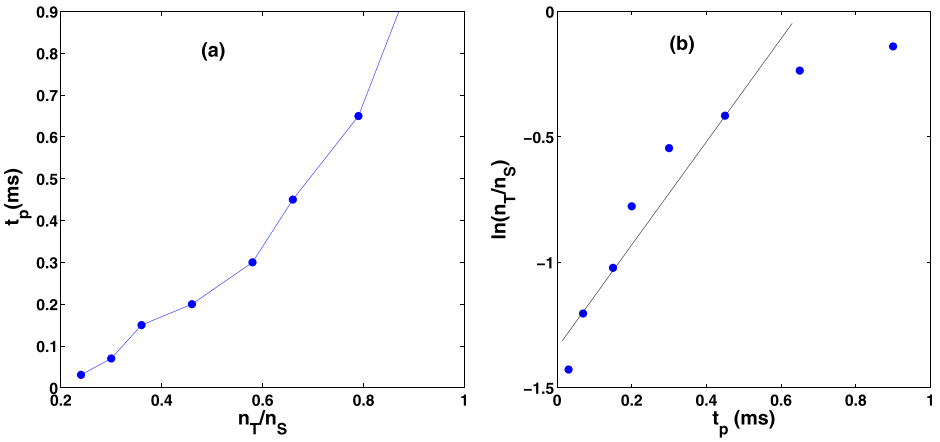


FIG. 6. (a) Increasing time period ($t_p$) as the function of the density ratio $n_T/n_S$ when FB voltage is maintained at 350 V. (b) Time period ($t_p$) versus logarithm of $n_T/n_S$ curve is fitted by a straight line indicating an underlying homoclinic bifurcation.

independent to each other. $0.5 < H < 1$ said to be persistent, and $0 < H < 0.5$ shows antipersistent time series. Fig. 5(b) represents the Hurst exponent of plasma potential fluctuations. The results presented in Fig. 5(b) indicate that the time series of plasma potential fluctuations exhibits an enhanced long range correlation with the variation of $n_T/n_S$. It is evident that more regular the dynamics, more higher is the value of the estimated Hurst exponent. It has been observed that as the density ratio is increased further, the regularity of the dynamics of the potential fluctuation is destroyed. This is consistence to the evidence obtained by using the normalized variance. Hence, both the quantifier Hurst exponent and normalized variance strongly reveal that $n_T/n_S$ decreases the persistence behaviour as well as regularity of the dynamics of the plasma potential fluctuation invoked at a constant fireball voltage.

Fig. 6(a) illustrates the relation between time period ($t_p$) and density ratio ($n_T/n_S$). It shows that time period is growing exponentially with the density ratio. However, in the low density ratio regime, the rise of the time period is less, but beyond a certain threshold value of $n_T/n_S = 0.36$, it increases abruptly and follows an exponential behavior. Fig. 6(b) shows the logarithmic plot of the time period versus $n_T/n_S$, and it represents power law relation with exponent 2.03. The positive scaling of the power law relation confirms the nature of homoclinic bifurcation, and it is evident that when $n_T/n_S$ increases, plasma density gradient starts to fall and compels the system to evolve from ordered to a complex state.

### B. Power spectral analysis and phase space plot

Power spectrum has been analyzed to gain an insight of the nonlinear dynamical phenomena of the system. Fig. 7 represents the power spectrum of the plasma fluctuations as shown in Fig. 4. Figs. 7(a), 7(b), and 7(c) show distinct and sharp peaks. With further increase of density ratio, about $n_T/n_S = 0.36$, the dominant frequency jumps to 26.4 kHz. After this $n_T/n_S$, a sudden fall in instability frequency has been observed in the system. When $n_T/n_S = 0.66$, distinct frequency of 6.8 kHz is observed. It is seen that as $n_T/n_S$ increases, the frequency bursts appear at $n_T/n_S = 0.79$ and are retained up to $n_T/n_S = 0.87$. The nature of this type of frequency bursts in the absence of fireball was discussed in detail by Sarma *et al.*[31] The enhancement of the density gradient in double plasma system is the cause of this ion acoustic instability when the density gradient is very high.

Fig. 8 shows phase space plot of the time series of plasma potential fluctuation. Figs. 8(a) and 8(b) show indistinguishable lobes having a beak like a bird, while at Fig. 9(f), one small lobe appears at $n_T/n_S = 0.36$ which corresponds to a homoclinic orbit. The orbit disappears with further increase of $n_T/n_S$. Similar abrupt changes have also been observed in spectral analysis. The lobe nature changes and it

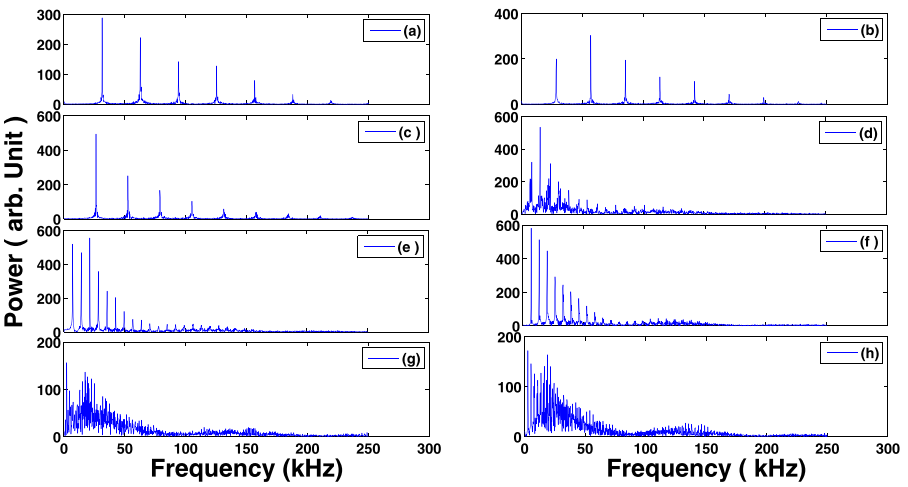


FIG. 7. Power spectrum of the raw signal of plasma potential fluctuations at different density ratios between source to target chamber: (a) 0.24, (b) 0.3, (c) 0.36, (d) 0.46, (e) 0.58, (f) 0.66, (g) 0.79, and (h) 0.87, when fireball voltage is 350 V.

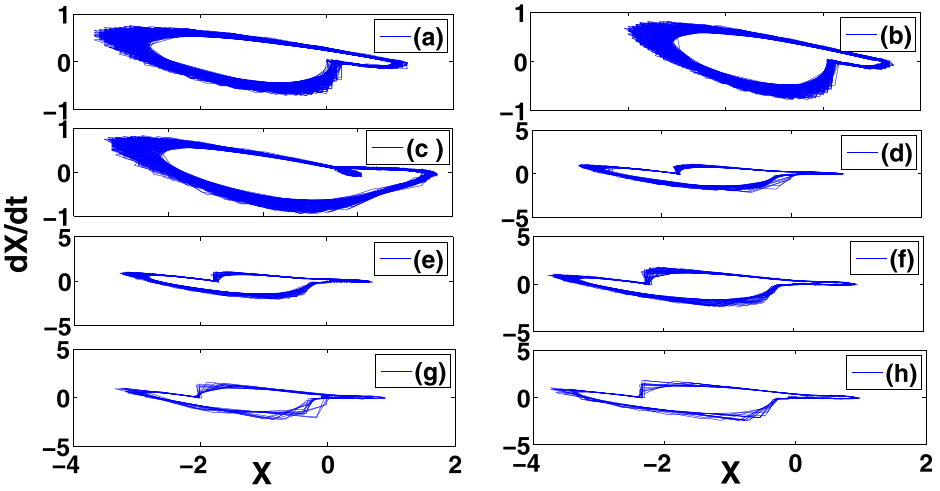


FIG. 8. Phase space plot of the plasma potential fluctuations at different values of $n_T/n_S$: (a) 0.24, (b) 0.3, (c) 0.36, (d) 0.46, (e) 0.58, (f) 0.66, (g) 0.79, and (h) 0.87 at 350 V fireball voltage.

appears like a bird, having a beak and tail. The lobe nature retains similarity up to $n_T/n_S = 0.87$.

## V. RECURRENCE PLOT

RP analysis of nonlinear time series is a relatively new and advanced technique introduced by Eckmann *et al.*[34] It is based on phase space reconstruction of a dynamical system, which besides giving visual information also has several measures to quantify various complexities associated with the different small scale recurrent structures. According to Taken's embedding theorem[35] using a time series data $X_i$, an embedding can be made using the vector $\vec{Y}_i = \vec{X}_i; \vec{X}_{i+\tau}; \vec{X}_{i+(d-1)\tau}$ where $d$ is the embedding dimension and $\tau$ is the time delay. The correct embedding parameters preserving the topological property of phase space are estimated by false nearest neighbor and mutual information method.[36,37] The original time series is now embedded into a d-dimensional reconstructed phase space. A recurrence is said to occur whenever a trajectory visits approximately the same region of phase space. The RP is a graphical representation of the square matrix

$$R_{i,j} = H(\epsilon - \|\vec{Y}_i - \vec{Y}_j\|), \quad i,j = 1,2,...N,$$

where $\epsilon$ is a predetermined threshold, $H$ is the Heaviside unit step function, and $N$ is the number of data points of the signal. Both the axes of the graph represent the temporal extent to which the signal spans. Several statistical measures are there to quantify the characteristics of the different structures appearing in a RP form a diagnostic tool known as RQA.[40] For example, the RQA measure determinism (*DET*) gives the ratio of the number of recurrence points in the diagonal lines to all the recurrence points. For deterministic dynamics, determinism (*DET*) is close to unity and approaches zero when the behavior is random. Other parameters related to diagonal lines such as average diagonal line length or Shannon entropy (*ENT*) of the probability distribution of the diagonal line lengths also reflect the complexity of the deterministic structures in the system. The longest diagonal $L_{max}$ in the RP is related to the exponential divergence of phase space trajectory.

### A. RQA of plasma oscillations

In order to get the instant overview of dynamical transition of the system, recurrence plot is constructed for each time series obtained for different $n_T/n_S$. Fig. 9 shows the recurrence plots of the oscillation of plasma potential fluctuations. The embedding dimension and delay are estimated to be around 3–4 and 4–30. The threshold value is taken up as 0.25. Fig. 9(a) reflects that RP points are trying to follow a diagonal line, as periodicity is present in the system. But the diagonal lines are small, and the distance between them

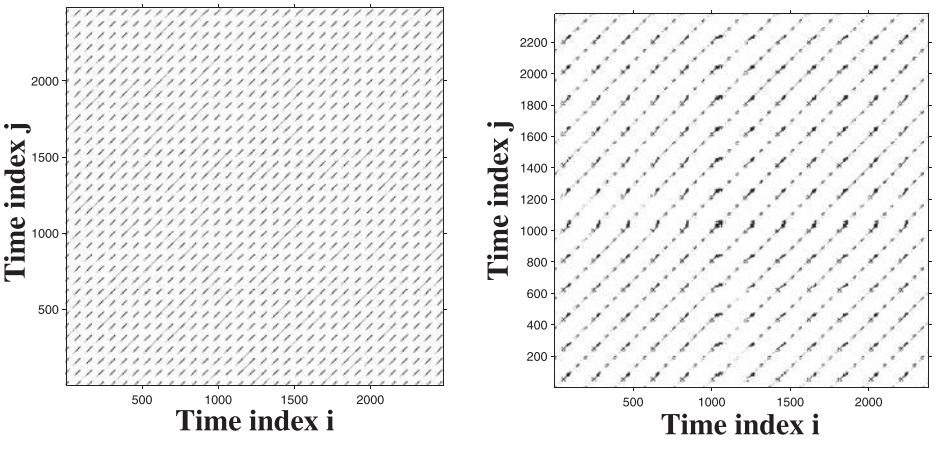


(a) (b)

FIG. 9. Recurrence plot of the plasma potential fluctuations at target to source density ratio $n_T/n_S$: (a) 0.24 and (b) 0.87.

is not equal. Hence, it reflects mixed oscillation. It is found that the distance between the diagonal lines is increasing gradually with the evolution of the system. However, the distance between the consecutive diagonal lines indicates time period of the system. Hence, time period of the oscillation is increasing with increasing $n_T/n_S$. It is clearly conjectured that homoclinic bifurcation is taking place in the system. Since target current is very less, potential at $n_T/n_S = 0.3$ and 0.36 is high because of diffused plasma.[31]

In Fig. 9(b), several small diagonal lines are observed, and the consecutive distance between the diagonal lines becomes broad. It conjectures the broadening of the interspike distance with the increase of the density ratio.

Fig. 10 shows the recurrence quantification variables, *viz.*, *DET*, $L_{max}$, and *ENT* with respect to the density ratio $n_T/n_S$. *DET*, $line_{max}$, and *ENT* values are displaying decreasing trend when density ratio is increasing as the oscillation is showing irregular to regular transition. The *DET* (determinism) is the measure of the predictability of the dynamical system, and it is based on the diagonals of the RP. It is defined as

$$DET = \frac{\sum_{l=l_{min}}^{N} lP(l)}{\sum_{l=1}^{N} lP(l)},$$

where $P(l)$ is the histogram of the diagonal lines of length $l$. The deterministic process causes noninterrupted diagonal lines and less single isolated recurrence points.[41] For a periodic system, *DET* value shows 1. Initially, the *DET* value is almost unity, and it starts to fall while the density ratio is increasing. However, a sudden jump is observed when the density ratio reaches 0.36. The jump is more prominent in the entropy plot. Hence, this particular density ratio plays a role of threshold density at which the bifurcation is taking place.

The quantifier *ENT*(entropy) indicates the Shanon entropy of the probability

$$p(l) = P(l)/N_l,$$

to find a diagonal line of exact length of $l$ in the RP. It is estimated by

$$ENT = -\sum_{l=l_{min}}^{N} p(l) lnp(l).$$

The variable entropy reflects the complexity of the oscillation through the distribution of the diagonal line. Entropy becomes maximum, if all diagonal lines are observed in the RP. It becomes minimum, if less diagonal lines are present. Thus, for the noisy, irregular, and random time series, the value of entropy is very less. RQA analysis is reflecting that in periodic regime, entropy becomes high as the large diversity in diagonal line length occurs.[40] It has been conjectured that the complexity of the system is increasing, when the density ratio is increasing as the entropy value is decreasing.

In general, inverse of $L_{max}$ is proportional to positive Lyapunov exponent. It is defined by

$$L_{max} = max((l_i)_{i=1}^{N_l}),$$

where

$$L = \frac{\sum_{l=l_{min}}^{N} lP(l)}{\sum_{l=l_{min}}^{N} P(l)}.$$

Hence, the small value of $L_{max}$ elucidates the chaotic or complex dynamics of plasma potential fluctuations, and the large value of $L_{max}$ reflects the inverse phenomena. Hence, $L_{max}$ reveals that complexity of the potential fluctuation increases with the increase of $n_T/n_S$.

### B. Skewness and kurtosis

The skewness quantifies the degree of asymmetry of a distribution around the mean data. There are few recent applications, where skewness and kurtosis are used to investigate the complexity of the raw data in glow discharge plasma system.[38,39] When a distribution looks same to both left and right from the center point, it can be considered as a symmetric distribution. If the value of skewness is negative, the data are concentrated more to the left of the mean than to the right and vise versa. The value of skewness of the normal distribution (Gaussian distribution) is always zero. Skewness of a distribution is given by

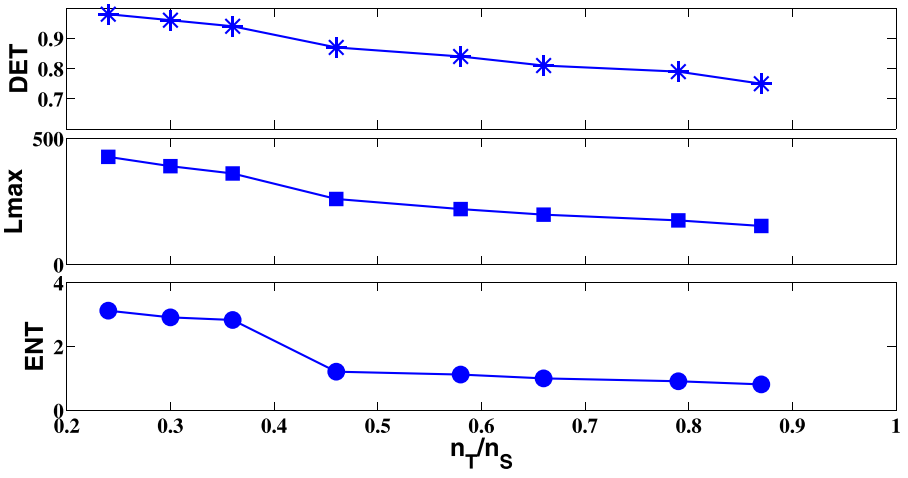


FIG. 10. Recurrence variables *DET*, $L_{max}$, and *ENTR* of the plasma potential fluctuations at various target to source density ratios ($n_T/n_S$).

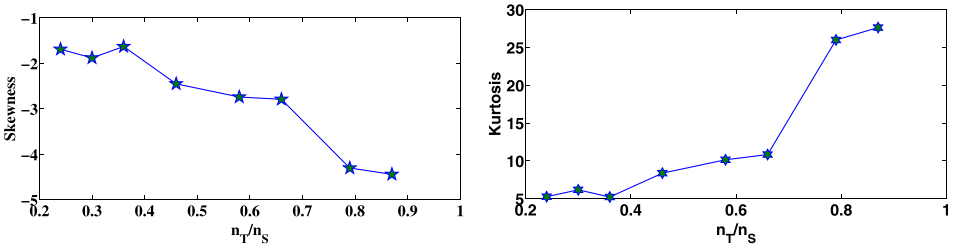


FIG. 11. (a) Skewness and (b) kurtosis of plasma potential fluctuations at different density ratio.

$$S = \frac{E[x-\mu]^3}{\sigma^3},$$

where $x$ is the data, $\mu$ is the mean of $x$, $\sigma$ is the standard deviation of $x$, and $E$ represents the expected value of the quantity.

Kurtosis elucidates the peakedness or flatness of a distribution of fluctuations around the data mean. A higher and lower value of kurtosis represents a sharper peak and flatter peak than normal distribution, with values concentrated around the mean of the distribution. The value of the kurtosis of the normal distribution is 3. Kurtosis of a distribution is given by

$$K = \frac{E[x-\mu]^4}{\sigma^4},$$

where $x$ is the data, $\mu$ is the mean of $x$, $\sigma$ is the standard deviation of $x$, and $E$ is the expected value of the quantity.

In Figs. 11(a) and 11(b), skewness and kurtosis are plotted with respect to the variation of $n_T/n_S$. The value of skewness is maximum $-1.69$ at $n_T/n_S = 0.24$. It has been observed that at $n_T/n_S = 0.87$ skewness of plasma potential fluctuations approaches to a minimum value of $-4.44$. It is seen that with the increase of $n_T/n_S$, skewness value has decreased.

Fig. 11(b) reflects that with the increase of $n_T/n_S$ value, kurtosis is increasing. When $n_T/n_S = 0.87$, kurtosis is showing the maximum value (27.62). The data distribution of target plasma current of the plasma potential fluctuation is becoming more peaked as the value of kurtosis is increasing with the variation of plasma density ratio. A sudden jump has been observed in both the values of skewness and kurtosis when $n_T/n_S$ is increased from 0.66 to 0.79.

## VI. FB EFFECTS AT CONSTANT $n_T/n_S$

The voltage applied to the fireball electrode is varied over a certain range of values to see the nonlinear behavior with the rise of fireball voltage at constant $n_T/n_S$. The experiment has been repeated for all values of $n_T/n_S$. Almost similar experiment was done by Chiriac *et al.*[42] in a single source plasma device for various voltages applied to the fireball electrode. However, in this report, effect of fireball has been observed for different values of $n_T/n_S$ in a DP device. It has been observed that when $n_T/n_S = 0.36$, significant changes have been taking place as discussed also in the earlier section. Hence, the time series of PPF observed at $n_T/n_S = 0.36$ for different fireball voltages is shown in Fig. 12(a). The oscillation of plasma potential fluctuation is presenting two large and one small oscillation at 280 V fireball voltage. One large oscillation disappears when the fireball voltage is increased to 290 V. Further increase of fireball voltage shows an appearance of a new large oscillation which sustains up to 310 V. The time series is showing the onset of inverse homoclinic bifurcation as the time period is decreasing with the increase of fireball voltage.

Fig. 12(b) is displaying its corresponding power spectrum. A broadband frequency range from 2 kHz to 123.4 kHz is observed in Fig. 11(a). In Fig. 12(b), several frequencies ranging from 6 kHz to 71 kHz are noticed. The frequencies are becoming distinct and sharp with fundamental frequency 22.6 kHz and 24.8 kHz, and spread up to 112.4 kHz at the fireball voltages 320 V and 330 V.

Fig. 13 shows the phase space plot of the floating potential fluctuation. The phase space plot looks like a bird having tail and beak. But the trend of the phase space plot is opposite to Fig. 8, as inverse homoclinic bifurcation is taking place with the increase of fireball voltage. The phase space

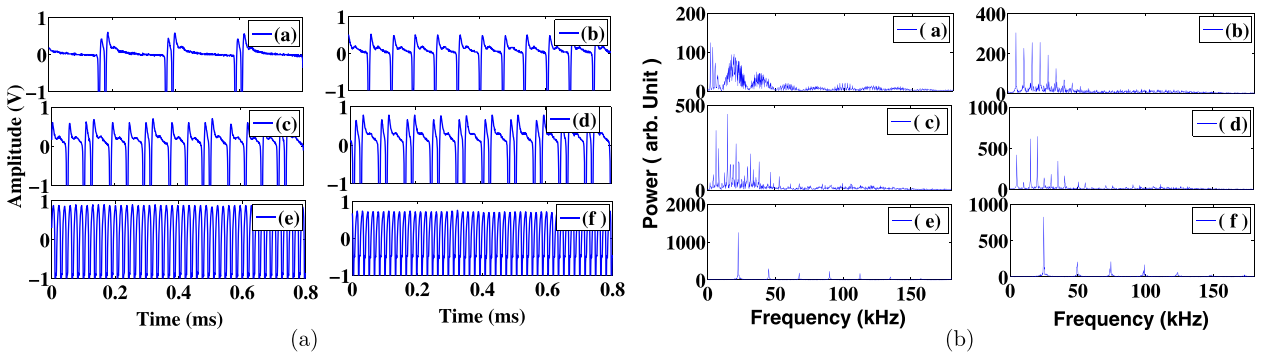


FIG. 12. (a) Time series and (b) power spectrum plot of plasma potential fluctuations at various fireball voltages: (a) 280 V, (b) 290 V, (c) 300 V, (d) 310 V, (e) 320 V, and (f) 330 V.

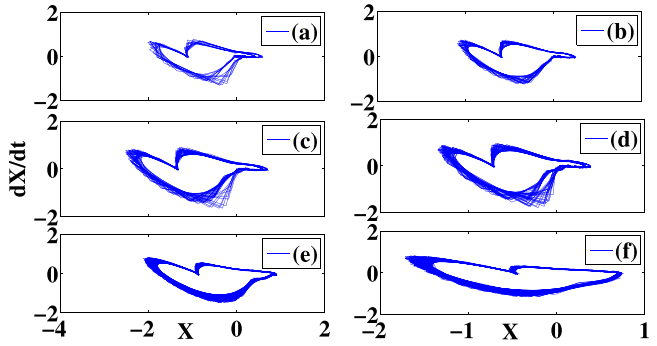


FIG. 13. Phase space plot of plasma potential fluctuations at various fireball voltages: (a) 280 V, (b) 290 V, (c) 300 V, (d) 310 V, (e) 320 V, and (f) 330 V.

plot is gradually going towards a round loop as the plasma potential fluctuation is moving from complex to order state.

Fig. 14 shows the experimental *NV* curve as a function of fireball voltage at a constant density ratio. The *NV* value of plasma oscillation decreases as the oscillation approaches to the bifurcation point. A sharp fall is observed at 310 V as the bifurcation is taking place, and the oscillation exhibits irregular to regular transition as the fireball voltage is further increased. This is the consequence of the dynamics provoked by the fireball.

Fig. 15(a) shows the skewness of plasma potential fluctuations. It has been noticed that skewness value is increasing with the increase of fireball voltage, and it becomes highest (0.78) at 330 V. However, in this case, it is showing almost linear relationship with the fireball voltage. Fig. 15(b) illustrates the kurtosis with respect to the discharge voltage applied to additional electrode, while kurtosis showing opposite trend. Kurtosis value is maximum around 18.45 at 280 V and minimum around 2.69 V at 330 V.

Fig. 16 shows the recurrence quantification variables, viz., *DET*, $L_{max}$, and *ENT* with respect to the fireball voltage. *DET* value is displaying an increasing trend due to the transition from irregular to ordered state. The signal is becoming more predictable with the increase of the fireball voltage. When the system shows periodic nature, the *DET* value becomes 1. In the present situation, *DET* value of 0.97 is obtained because of the presence of noise. $L_{max}$ and entropy are also showing similar increasing trend with the change of fireball voltage.

## VII. THEORY AND NUMERICAL MODELLING

The temporal behaviour of plasma oscillations observed in the bulk plasma is closely connected with the fireball dynamics. The observed relaxation oscillations are due to the compressive ion sound pulses generated by the disruption in the double layer that forms the boundary of the fireball. The bulk plasma oscillations show normal and inverse homoclinic bifurcation, respectively, with the change in the target to source density and fireball voltage. With increase of fireball voltage, size of the fireball increases leading to a more

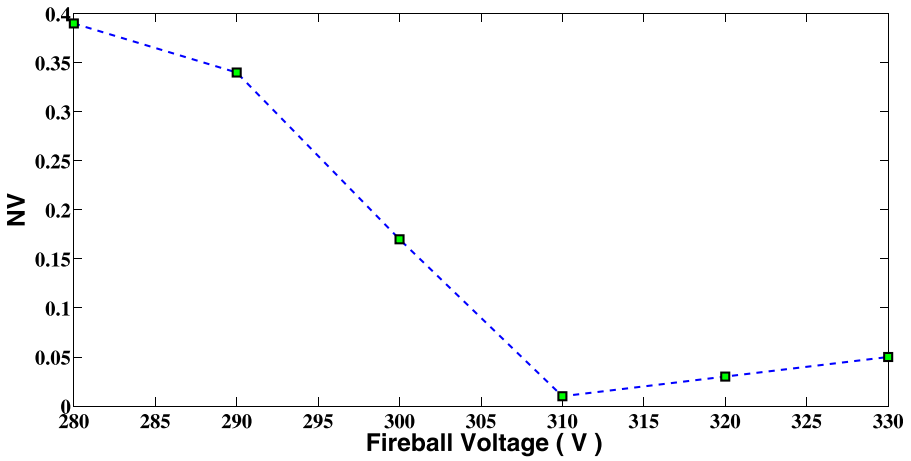


FIG. 14. Normalized variance for plasma potential fluctuations in various fireball voltages at $n_T/n_S = 0.36$.

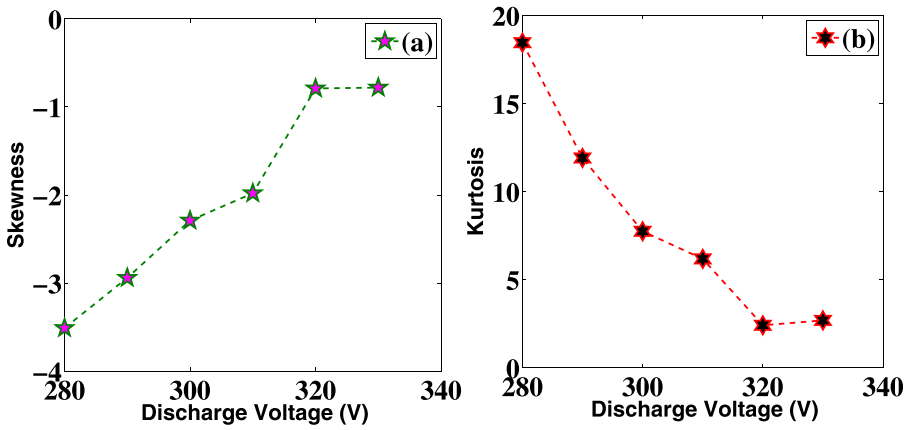


FIG. 15. (a) Skewness and (b) kurtosis of plasma potential fluctuations at various fireball voltages: (1) 280 V, (2) 290 V, (3) 300 V, (4) 310 V, (5) 320 V, and (6) 330 V.

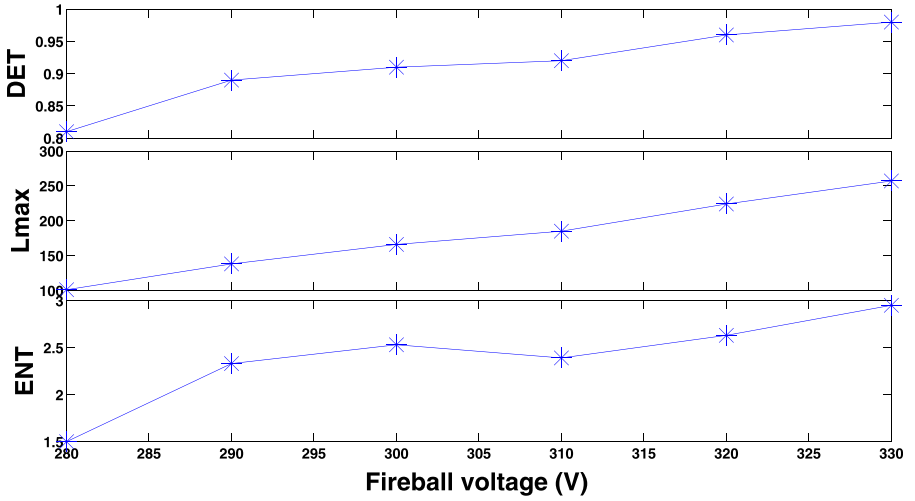


FIG. 16. Recurrence variables *DET*, $L_{max}$, and *ENT* of the plasma potential fluctuations at various fireball voltages.

frequent formation and disruption of fireball dynamics. The converse occurs with increase in the plasma target density, for a given fireball voltage.

To validate the experimental observations of homoclinic bifurcation, an analytical model has been initiated based on two-fluid equation developed by Kadji *et al.*[43] Recently, the equation has also been considered for studying various nonlinear dynamical phenomena in a glow discharge plasma.[29,44]

$$\ddot{x} + (a + e + bx + cx^2)\dot{x} + x + a\left(ex + \frac{b}{2}x^2 + \frac{c}{3}x^3\right) = 0, \tag{1}$$

where $x$ denotes the amplitude of plasma potential fluctuations, and all variations are considered with respect to time normalized to ion acoustic frequency. Equation (1) is solved numerically with initial conditions of $x_0 = 1$ and $\dot{x}_0 = 1$. The parameters $a$, $b$, and $c$ are considered as follows:

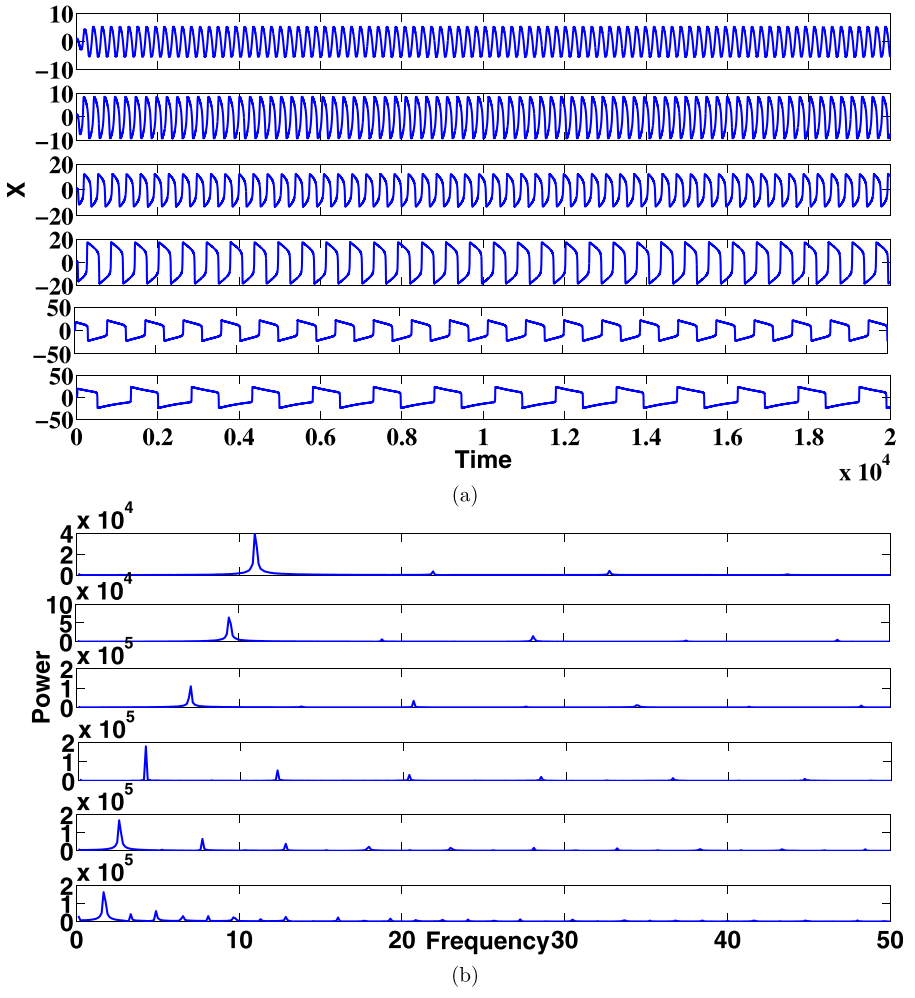


FIG. 17. (a) Numerical solutions and (b) corresponding power spectra plot for various values of $e$: (a) −0.8, (b) −2, (c) −4, (d) −8, (e) −12, and (f) −14.65.

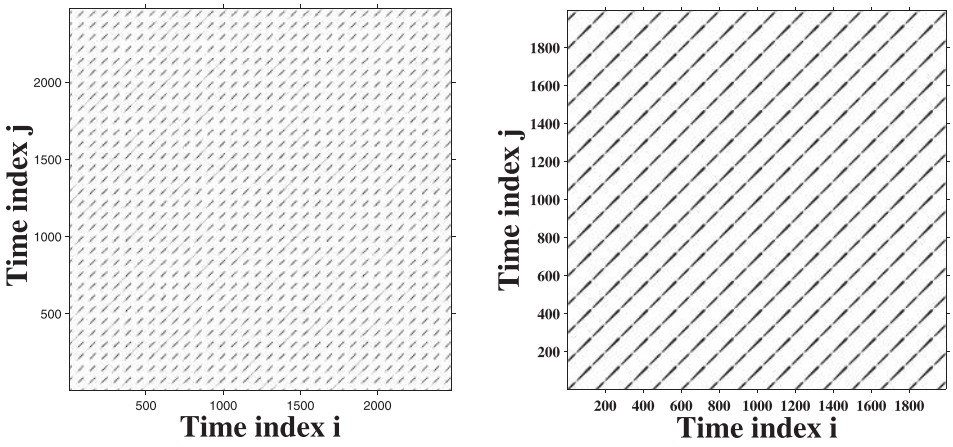


(a) (b)

FIG. 18. Recurrence plot for numerical solutions at different values of $e$: (a) $e = -0.8$ and (b) $e = -14.65$.

$a = b = c = 0.1$. Here $a$, $b$, $c$, and $e$ denote the collision term, 2-body and 3-body recombination, and the ionization effects, respectively. Figs. 17(a) and 17(b) show time series for various values of $e$ and the corresponding power spectrum. The model describes the increase in the ratio of target to source density through the introduction of the ionization term $e$. Increase of $e$ is assumed to increase the target density.

At $e = -0.8$, periodic oscillations have been observed. The time period of oscillations is gradually increasing when value of $e$ increases gradually from $-0.8$ to $-14.65$. The broadening of the time period with respect to the enhancement of ionisation supports the homoclinic bifurcation. Fig. 17(b) shows at $e = -0.8$ that sharp spike is present. When $e$ increases to $e = -14.65$, one large peak associated with several closely spaced small peaks is observed. Fig. 18 presents recurrence plot of numerical solutions when $e = -0.8$ and $e = -14.65$. The RPs resemble the experimental result. It is clearly seen that the vertical distance between the consecutive diagonal line increases, which elucidates the homoclinic behaviour of the plasma oscillation through the broadening of the time period.

## VIII. CONCLUSION

We have investigated the appearance of homoclinic and inverse homoclinic bifurcation in the presence of fireball in a low temperature double plasma system. It has been found that charged particle density gradient and the appearance of plasma fireball cause drastic change in the dynamical scenario of plasma oscillations. Identification of homoclinic bifurcation is made using recurrence quantification analysis, spectral analysis, skewness, and kurtosis, respectively. It is noticed that with the rise of density ratio, density gradient is developing in the system with the simultaneous appearance of homoclinic bifurcation phenomena in the plasma oscillations. However, when positive voltage is applied to the additional electrode, electrons are drawn towards the electrode accompanied by the ions and form a layer of glowing region named as fireball. With the increase of the fireball voltage, more electrons are accelerated to the electrode and local ionization is increasing, and as a result, sheath region is also enhancing. At a constant density ratio when FB voltage is gradually increasing, electron rich sheath develops near the electrode that repels the ions. The enhancement of the sheath excites inverse homoclinic bifurcation in the dynamics of the plasma potential fluctuations. However, it has been noticed that it needs more voltage to produce fireball in high density ratio compared to low density ratio.

Recurrence plot is a novel tool for nonlinear time series analysis. In RP, the distance between two consecutive diagonal lines is increasing which is strongly indicative of the occurrence of homoclinic bifurcation. The time period of plasma oscillation is following an exponential scaling law that strongly conjectures the occurrence of homoclinic behaviour in the double plasma system.

A numerical modelling has been carried out to explore the influence of fireball in the dynamical transition of the double plasma system. It has been noticed that while increasing the discharge voltage, ionization is also increasing and the oscillations are becoming more ordered. The visual change displayed in RP also reveals, the increase of the time period as a function of density ratio, confirming the occurrence of homoclinic bifurcation phenomena. Hence, from both experimental and theoretical results, it can be elucidated that the fireball is playing a vital role for the appearance of homoclinic bifurcation in the double plasma system.

## ACKNOWLEDGMENTS

The authors wish to thank R. Schrittwieser and C. Ionita, Innsbruck University, Innsbruck, Austria, for providing the experimental facility. The authors would like to acknowledge the referee for their valuable suggestions to improve the quality of the paper. Authors are also thankful to BRNS-DAE, Government of India, for providing the financial support through the project grant (Ref. No. 2013/34/29/BRNS).

[1]T. Gyergyek, M. Cercek, R. Schrittwieser, and C. Ionita, Contrib. Plasma Phys. **42**, 508 (2002).
[2]D. G. Dimitru, M. Aflori, L. M. Ivan, C. Ionita, and R. W. Schrittwieser, Plasma Phys. Controlled Fusion **49**, 237 (2007).
[3]R. L. Stenzel, C. Ionita, and R. Schrittwieser, Plasma Sources Sci. Technol. **17**, 035006 (2008).
[4]C. Ionita, D. Dimitriu, and R. Schrittwieser, Int. J. Mass. Spectrom. **233**, 343 (2004).
[5]R. L. Stenzel, C. Ionita, and R. Schrittwieser, J. Appl. Phys. **109**, 113305 (2011).
[6]R. L. Stenzel, J. Gruenwald, B. Fonda, C. Ionita, and R. Schrittwieser, Phys. Plasmas **18**, 012104 (2011).

[7]R. L. Stenzel, J. Gruenwald, B. Fonda, C. Ionita, and R. Schrittwieser, Phys. Plasmas **18**, 012105 (2011).
[8]T. Gyergyek, Plasma Phys. Controlled Fusion **41**, 175 (1999).
[9]H. M. Mott-Smith and I. Langmuir, Phys. Rev. **28**, 727 (1926).
[10]K. U. Riemann, J. Phys. D: Appl. Phys. **24**, 493 (1991).
[11]I. Langmuir, Science **58**, 290 (1923).
[12]S. Torven and D. Andersson, J. Phys. D: Appl. Phys. **12**, 717 (1979).
[13]T. An, R. L. Merlino, and N. D'Angelo, J. Phys. D: Appl. Phys. **27**, 1906 (1994).
[14]D. D. Tskhakaya, F. Binte-E-Munir, and S. Kuhn, J. Plasma Phys. **76**, 559 (2010).
[15]A. C. Calder and J. G. Laframboise, Phys. Fluids B **2**, 655 (1990).
[16]A. C. Calder, W. Hulbert, and J. G. Laframboise, Phys. Fluids B **5**, 674 (1993).
[17]J. M. Urrutia and R. L. Stenzel, Phys. Plasmas **4**, 36 (1997).
[18]P. A. Miller and M. E. Riley, J. Appl. Phys. **82**, 3689 (1997).
[19]R. L. Stenzel, Phys. Fluids B **1**, 2273 (1989).
[20]Yu. P. Bliokh, J. Feltsteiner, and Ya. Z. Slutsker, Europhys. Lett. **46**, 735 (1999).
[21]D. D. Blackwell, D. N. Walker, S. J. Messer, and W. E. Amatucci, Phys. Plasmas **12**, 093510 (2005).
[22]K. G. Emeleus, Int. J. Electron. **56**, 441 (1984).
[23]M. Sanduloviciu and E. Lozneanu, Plasma Phys. Controlled Fusion **28**, 585 (1986).
[24]L. Conde and L. Leon, Phys. Plasmas **1**, 2441 (1994).
[25]V. N. Belykh, I. V. Belykh, M. Colding-Jorgensen, and E. Mosekilde, Eur. Phys. J. E **3**, 205 (2000).
[26]G. J. E. Santos, M. Rivera, M. Eiswirth, and P. Parmananda, Phys. Rev. E **70**, 021103 (2004).
[27]Md. Nurujjaman, A. N. Sekar Iyengar, and P. Parmananda, Phys. Rev. E **78**, 026406 (2008).
[28]B. Krauskopfa, K. Schneider, J. Sieber, S. Wieczorekc, and M. Wolfrum, Opt. Commun. **215**, 367 (2003).
[29]D. Saha, P. K. Shaw, M. S. Janaki, A. N. Sekar Iyengar, S. Ghosh, V. Mitra, and A. M. Wharton, Phys. Plasmas **21**, 032301 (2014).
[30]J. Masel and H. L. Swinney, J. Chem. Phys. **85**, 6430 (1986).
[31]A. Sarma, H. Bailung, and J. Chutia, Phys. Plasmas **4**, 61 (1997).
[32]B. B. Mandelbort and J. R. Wallis, Water Resour. Res. **5**, 321, doi:10.1029/WR005i002p00321 (1969).
[33]B. A. Carreras *et al.*, Phys. Plasmas **5**, 3632 (1998).
[34]J.-P. Eckmann, S. O. Kamphorst, and D. Ruelle, Europhys. Lett. **4**, 973 (1987).
[35]F. Takens, *Lecture Notes in Mathematics* (Springer, 1981), Vol. 898, p. 366.
[36]A. M. Fraser and H. L. Swinney, Phys. Rev. A **33**, 1134 (1986).
[37]S. Schinkel, N. Marwan, O. Dimigen, and J. Kurths, Phys. Lett. A **373**, 2245 (2009).
[38]V. Mitra, A. Sarma, M. S. Janaki, A. N. Sekar Iyengar, B. Sarma, N. Marwan, J. Kurths, P. K. Shaw, D. Saha, and S. Ghosh, Chaos, Solitons Fractals **69**, 285 (2014).
[39]A. M. Wharton, A. N. Sekar Iyenger, and M. S. Janaki, Phys. Plasmas **20**, 022301 (2013).
[40]L. L. Trulla, A. Giuliani, J. P. Zbilut, and C. L. Webber, Jr., Phys. Lett. A **223**, 255 (1996).
[41]N. Marwan, M. C. Romano, M. Thiel, and J. Kurths, Phys. Rep. **438**, 237 (2007).
[42]S. Chiriac, D. G. Dimitriu, and M. Sanduloviciu, Phys. Plasmas **14**, 072309 (2007).
[43]E. Kadji, N. Benjou, C. Orou, and P. K. Talla, Phys. Plasmas **15**, 032308 (2008).
[44]S. Ghosh, P. K. Shaw, A. N. Sekar Iyengar, M. S. Janaki, D. Saha, A. M. Wharton, and V. Mitra, Phys. Plasmas **21**, 032303 (2014).